

Finite-size Scaling of $O(n)$ Systems at the Upper Critical Dimensionality*

Jian-Ping Lv,^{1,†} Wanwan Xu,¹ Yanan Sun,¹ Kun Chen,^{2,‡} and Youjin Deng^{3,4,§}

¹*Department of Physics, Anhui Key Laboratory of Optoelectric Materials Science and Technology, Key Laboratory of Functional Molecular Solids, Ministry of Education, Anhui Normal University, Wuhu, Anhui 241000, China*

²*Department of Physics and Astronomy, Rutgers, The State University of New Jersey, Piscataway, New Jersey 08854-8019*

³*National Laboratory for Physical Sciences at Microscale and Department of Modern Physics, University of Science and Technology of China, Hefei, Anhui 230026, China*

⁴*Department of Physics and Electronic Information Engineering, Minjiang University, Fuzhou, Fujian 350108, China*

(Dated: September 23, 2020)

Logarithmic finite-size scaling of the $O(n)$ universality class at the upper critical dimensionality ($d_c = 4$) has a fundamental role in statistical and condensed-matter physics and important applications in various experimental systems. Here, we address this long-standing problem in the context of the n -vector model ($n = 1, 2, 3$) on periodic four-dimensional hypercubic lattices. We establish an explicit scaling form for the free energy density, which simultaneously consists of a scaling term for the Gaussian fixed point and another term with multiplicative logarithmic corrections. In particular, we conjecture that the critical two-point correlation $g(r, L)$, with L the linear size, exhibits a two-length behavior: following the behavior r^{2-d_c} governed by Gaussian fixed point at shorter distance and entering a plateau at larger distance whose height decays as $L^{-d_c/2}(\ln L)^{\hat{p}}$ with $\hat{p} = 1/2$ a logarithmic correction exponent. Using extensive Monte Carlo simulations, we provide complementary evidence for the predictions through the finite-size scaling of observables including the two-point correlation, the magnetic fluctuations at zero and non-zero Fourier modes, and the Binder cumulant. Our work sheds light on the formulation of logarithmic finite-size scaling and has practical applications in experimental systems.

Keywords: critical phenomena; universality class; $O(n)$ vector model; finite-size scaling

I. INTRODUCTION

The $O(n)$ model of interacting vector spins is a much-applied model in condensed-matter physics and one of the most significant classes of lattice models in equilibrium statistical mechanics [1, 2]. The Hamiltonian of the $O(n)$ vector model is written as

$$\mathcal{H} = - \sum_{\langle \mathbf{r}\mathbf{r}' \rangle} \vec{S}_{\mathbf{r}} \cdot \vec{S}_{\mathbf{r}'}, \quad (1)$$

where $\vec{S}_{\mathbf{r}}$ is an n -component isotropic spin with unit length and the summation runs over nearest neighbors. Prominent examples include the Ising ($n = 1$), XY ($n = 2$) and Heisenberg ($n = 3$) models of ferromagnetism, as well as the self-avoiding random walk ($n \rightarrow 0$) in polymer physics. Its experimental realization is now available for various n values in magnetic materials [3–7], superconducting arrays [8, 9] and ultracold atomic systems [10, 11].

Finite-size scaling (FSS) is an extensively utilized method for studying systems of continuous phase transitions [12], including the $O(n)$ vector model (1). Near criticality, these systems are characterized by a diverging correlation length

$\xi \propto t^{-\nu}$, where parameter t measures the deviation from the critical point and ν is a critical exponent. For a finite box with linear size L , the standard FSS hypothesis assumes that ξ is bounded by the linear size L , and thus predicts that the singular part $f(t, h)$ of free energy density scales as

$$f(t, h) = L^{-d} \tilde{f}(tL^{y_t}, hL^{y_h}) \quad (2)$$

where \tilde{f} is a universal scaling function, t and h represent the thermal and magnetic scaling fields, and $y_t = 1/\nu$ and y_h are the corresponding thermal and magnetic renormalization exponents, respectively. Further, the standard FSS theory hypothesizes that at criticality, the spin-spin correlation function $g(r, L) \equiv \langle \vec{S}_0 \cdot \vec{S}_{\mathbf{r}} \rangle$ of distance r decays as

$$g(r, L) \asymp r^{-(d-2+\eta)} \tilde{g}(r/L), \quad (3)$$

where η relates to y_h by the scaling relation $\eta = 2 + d - 2y_h$. From (2) and (3), the FSS of various macroscopic physical quantities can be obtained. For instance, from the second derivative of $f(t, h)$ with respect to t or h , it is derived that at criticality, the specific heat behaves as $C \asymp L^{2y_t-d}$ and the magnetic susceptibility diverges as $\chi \asymp L^{2y_h-d}$. The FSS of χ can also be calculated by summing $g(r, L)$ over the system. Further, the thermodynamic critical exponents can be obtained by the (hyper-)scaling relations. For instance, in the thermodynamic limit ($L \rightarrow \infty$), the specific heat and the magnetic susceptibility scale as $C \propto t^{-\alpha}$ and $\chi \propto t^{-\gamma}$, where the critical exponents are $\alpha = 2 - d/y_t$ and $\gamma = (2y_h - d)/y_t$.

The $O(n)$ model exhibits an upper critical dimensionality $d_c = 4$ such that the thermodynamic scaling in higher dimensions $d > d_c$ are governed by the Gaussian fixed point, which has the critical exponents $\alpha = 0$ and $\gamma = 1$ etc. In the framework of renormalization group, the renormalization exponents

* Author Contributions: J.-P.L., K.C., and Y.D. designed the research and established the formulae for finite-size scaling. J.-P.L., W.X., and Y.S. performed simulations. J.-P.L., W.X., Y.S., and Y. D. analyzed the results. J.-P.L. and Y.D. wrote the manuscript. All the authors participated in the revisions of the manuscript.

† jplv2014@ahnu.edu.cn

‡ chenkun0228@gmail.com

§ yjdeng@ustc.edu.cn

near the Gaussian fixed point are

$$y_t = 2 \quad \text{and} \quad y_h = 1 + d/2 \quad (4)$$

for $d > d_c$.

Accordingly, the standard FSS formulae (2) and (3) predict that the critical susceptibility diverges as $\chi \asymp L^{2y_h-d} = L^2$ for $d > d_c$. However, for the Ising model on 5d periodic hypercubes, χ was numerically observed to scale as $L \asymp L^{5/2}$ instead of L^2 [13–18]. The FSS for $d \geq d_c$ turns out to be surprisingly subtle and remains a topic of extensive controversy [13–21].

It was realized that for $d > d_c$, the Gaussian exponents y_t and y_h in (4) can be renormalized by the leading irrelevant thermal field with exponent $y_u = 4 - d$ as [22–25]

$$y_t^* = y_t - \frac{y_u}{2} = \frac{d}{2} \quad \text{and} \quad y_h^* = y_h - \frac{y_u}{4} = \frac{3d}{4}, \quad (5)$$

and the FSS of the free energy density $f(t, h)$ becomes

$$f(t, h) = L^{-d} \tilde{f}(tL^{y_t^*}, hL^{y_h^*}). \quad (6)$$

In this scenario of dangerously irrelevant field, the FSS of the critical susceptibility becomes $\chi \asymp L^{2y_h^*-d} = L^{d/2}$, consistent with the numerical results [13–15, 17, 18]. It was further assumed that the scaling behavior of $g(r, L)$ is modified as [16]

$$g(r, L) \asymp r^{-(d-2+\eta_Q)} \tilde{g}(r/L) \quad (7)$$

with $\eta_Q = 2 - d/2$, such that the decay of $g(r, L)$ is no longer Gaussian-like. In the study of the 5d Ising model [13], a more subtle scenario was proposed that $g(r, L)$ decays as r^{-3} at short distance, gradually becomes $r^{-5/2}$ for large distance and has a crossover behavior in between. The introduction of η_Q was refuted by [15] as the magnetic fluctuations at non-zero Fourier mode $\mathbf{k} \neq 0$ scale as $\chi_{\mathbf{k}} \asymp L^2$ and underlined in [17] which revealed that the non-zero Fourier moments are governed by the Gaussian fixed point instead of being contaminated by the dangerously irrelevant field.

Using random-current and random-path representations [26–28], Papathanakos conjectured that the scaling behavior of $g(r, L)$ has a two-length form as [19]

$$g(r, L) \asymp \begin{cases} r^{-(d-2)}, & r \leq \mathcal{O}(L^{d/[2(d-2)]}) \\ L^{-d/2}, & r \geq \mathcal{O}(L^{d/[2(d-2)]}) \end{cases}. \quad (8)$$

According to (8), the critical correlation function still decays as Gaussian-like, $g(r, L) \asymp r^{-(d-2)}$, up to a length scale $\xi_1 = L^{d/[2(d-2)]}$, and then enters an r -independent plateau whose height vanishes as $L^{-d/2}$. Since the length ξ_1 is vanishingly small compared to the linear size, $\xi_1/L \rightarrow 0$, the plateau effectively dominates the scaling behavior of $g(r, L)$ and the FSS of χ . The two-length scaling form (8) has been numerically confirmed for the 5d Ising model and self-avoiding random walk, with a geometric explanation based on the introduction of unwrapped length on torus [18]. It is also consistent with the rigorous calculations for the so-called random-length random-walk model [20]. It is noteworthy that the two-length

scaling is able to explain both the FSS $\chi_0 \equiv \chi \asymp L^{5/2}$ for the susceptibility (the magnetic fluctuations at zero Fourier mode) [14] and the FSS $\chi_{\mathbf{k}} \asymp L^2$ for the magnetic fluctuations at non-zero modes [15, 17].

Combining all the existing numerical and (semi-)analytical insights [13–20], one of us and coworkers extended the scaling (6) of the free energy to be [21]

$$f(t, h) = L^{-d} \tilde{f}_0(tL^{y_t^*}, hL^{y_h^*}) + L^{-d} \tilde{f}_1(tL^{y_t^*}, hL^{y_h^*}), \quad (9)$$

where (y_t, y_h) are the Gaussian exponents (4) and (y_t^*, y_h^*) are still given by (5). Conceptually, scaling formula (9) explicitly points out the coexistence of two sets of exponents (y_t, y_h) and (y_t^*, y_h^*) , which was implied in previous studies [15, 17, 18, 20]. Moreover, a simple perspective of understanding was provided [21] that the scaling term with \tilde{f}_1 can be regarded to correspond to the FSS of the critical $O(n)$ model on a finite complete graph with the number of vertices $V = L^d$. As a consequence, the exponents (y_t^*, y_h^*) can be directly obtained from exact calculations of the complete-graph $O(n)$ vector model, which also gives $y_t^* = d/2$ and $y_h^* = 3d/4$. From this correspondence, the plateau of $g(r, L)$ in (8) is in line with the FSS of the complete-graph correlation function $g_{i \neq j} \equiv \langle \vec{S}_i \cdot \vec{S}_j \rangle$, which also decays as $V^{-1/2} = L^{-d/2}$. Note that, as a counterpart of the complete-graph scaling function, the term with \tilde{f}_1 should not describe the FSS of quantities merely associated with r -dependent behaviors, including magnetic/energy-like fluctuations at non-zero Fourier modes. Therefore, in comparison with (6), the scaling formula (9) can give the FSS of a more exhaustive list of physical quantities. The following gives some examples at criticality.

- let $\vec{M} \equiv \sum_{\mathbf{r}} \vec{S}_{\mathbf{r}}$ specify the total magnetization of a spin configuration, and measure its ℓ moment as $M_{\ell} \equiv \langle |\vec{M}|^{\ell} \rangle$. Equation (9) predicts $M_{\ell} \sim L^{\ell y_h^*} + qL^{y_h}$, with q a non-universal constant. In particular, the magnetic susceptibility $\chi_0 \equiv L^{-d} M_2 \asymp L^{d/2} [1 + \mathcal{O}(L^{(4-d)/2})]$, where the FSS from the Gaussian term \tilde{f}_0 is effectively a finite-size correction but its existence is important in analyzing numerical data [21].
- let $\vec{M}_{\mathbf{k}} \equiv \sum_{\mathbf{r}} \vec{S}_{\mathbf{r}} e^{i\mathbf{k} \cdot \mathbf{r}}$ specify the Fourier mode of magnetization with momentum $\mathbf{k} \neq 0$, and measure its ℓ moment as $M_{\ell, \mathbf{k}} \equiv \langle |\vec{M}_{\mathbf{k}}|^{\ell} \rangle$. The magnetic fluctuations at $\mathbf{k} \neq 0$ behaves as $\chi_{\mathbf{k}} \equiv L^{-d} M_{2, \mathbf{k}} \sim L^{2y_h-d} = L^2$. The behaviors of χ_0 and $\chi_{\mathbf{k}}$ have been confirmed for the 5d Ising model [15, 17, 18, 20].
- the Binder cumulant $Q \equiv \langle |\vec{M}|^2 \rangle^2 / \langle |\vec{M}|^4 \rangle$ should take the complete-graph value, as expected from the correspondence between the term with \tilde{f}_1 in (9) and the complete-graph FSS. For the Ising model, the complete-graph calculations give $Q = 4[\frac{\Gamma(3/4)}{\Gamma(1/4)}]^2 \approx 0.456947$, consistent with the 5d result in Ref. [13].

Analogously, the FSS behaviors of energy density, its higher-order fluctuations and the ℓ -moment Fourier modes at $\mathbf{k} \neq 0$ can be derived from (9).

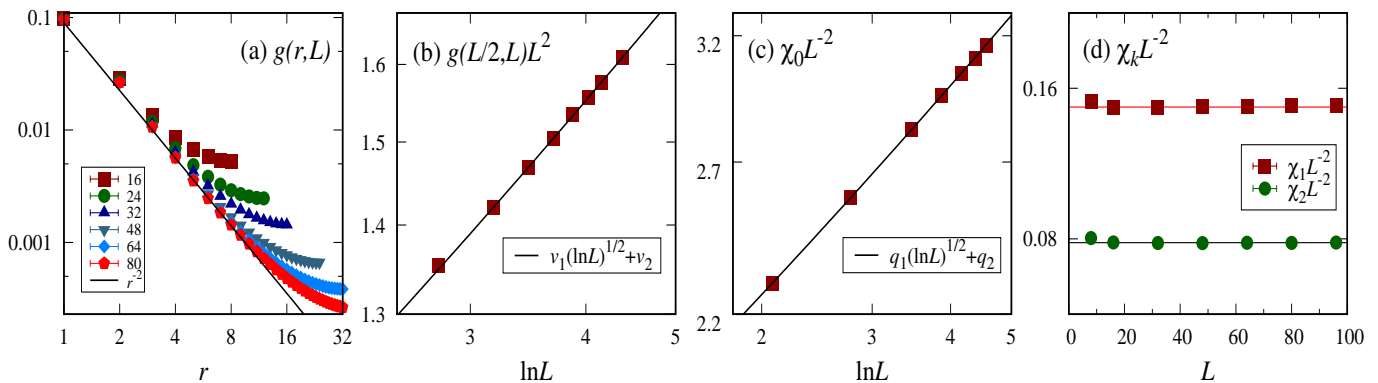


Figure 1. Evidence for conjectured formulae (11) and (12) in the example of the critical 4d XY model. (a) correlation function $g(r, L)$ in a log-log scale. The solid line stands for the r^{-2} behavior. (b) scaled correlation $g(r, L)L^2$ with $r = L/2$ versus $\ln L$ in a log-log scale. Thus, the horizontal axis is effectively in a double logarithmic scale of L . The solid line represents logarithmic divergence with $\hat{p} = 1/2$. (c) scaled magnetic susceptibility $\chi_0 L^{-2}$ versus $\ln L$ in a log-log scale. The solid line accounts for logarithmic divergence with $\hat{p} = 1/2$. (d) scaled $\mathbf{k} \neq 0$ magnetic fluctuations $\chi_1 L^{-2}$ and $\chi_2 L^{-2}$, with $\mathbf{k}_1 = (2\pi/L, 0, 0, 0)$ and $\mathbf{k}_2 = (2\pi/L, 2\pi/L, 0, 0)$, respectively. The horizontal lines strongly indicate the absence of logarithmic corrections in the scaling of χ_k .

We expect that the FSS formulae (8) and (9) are valid not only for the $O(n)$ vector model but also for generic systems of continuous phase transitions at $d > d_c$. An example is given for percolation that has $d_c = 6$. It was observed [29] that at criticality, the probability distributions of the largest-cluster size follow the same scaling function for 7d periodic hypercubes and on the complete graph.

In this work, we focus on the FSS for the $O(n)$ vector model at the upper critical dimensionality $d = d_c$. In this marginal case, it is known that multiplicative and additive logarithmic corrections would appear in the FSS. However, exploring these logarithmic corrections turns out to be of notorious hardness. The challenge comes from the lack of analytical insights, the existence of slow finite-size corrections, as well as the unavailability of very large system sizes in simulations of high-dimensional systems.

For the $O(n)$ vector model, establishing the precise FSS form at $d = d_c$ is not only of fundamental importance in statistical mechanics and condensed-matter physics, but also of practical relevance due to the direct experimental realizations of the model, particularly in three-dimensional quantum critical systems [3–6, 10, 11]. For instance, to explore the stability of Anderson-Higgs excitation modes in systems with continuous symmetry breaking ($n \geq 2$), a crucial theoretical question is whether or not the Gaussian r -dependent behavior $g(r) \asymp r^{-2}$ is modified by some multiplicative logarithmic corrections.

II. SUMMARY OF MAIN FINDINGS

At the upper critical dimensionality ($d_c = 4$) of the $O(n)$ model, the state-of-the-art applications of FSS are mostly restricted to a phenomenological scaling form proposed by Kenna [30] for the singular part of free energy density, which was extended from Aktekin’s formula for the Ising

model [31],

$$f(t, h) = L^{-4} \tilde{f}(tL^{y_t}(\ln L)^{\hat{y}_t}, hL^{y_h}(\ln L)^{\hat{y}_h}) \quad (10)$$

for $n \geq 0$ and $n \neq 4$, where the renormalization exponents $y_t = 2$ and $y_h = 3$ are given by (4). Further, the renormalization-group calculations predicted the logarithmic-correction exponents as $\hat{y}_t = \frac{4-n}{2n+16}$ and $\hat{y}_h = 1/4$ [32, 33]. The leading FSS of χ_0 is hence given by $\chi_0 \asymp L^2(\ln L)^{1/2}$, independent of n .

Motivated by the recent progress for the $O(n)$ models for $d > d_c$ [15–21], we hereby propose that at $d = d_c$, the scaling form (10) for free energy should be revised as

$$f(t, h) = L^{-4} \tilde{f}_0(tL^{y_t}, hL^{y_h}) + L^{-4} \tilde{f}_1(tL^{y_t}(\ln L)^{\hat{y}_t}, hL^{y_h}(\ln L)^{\hat{y}_h}), \quad (11)$$

and the critical two-point correlation $g(r, L)$ behaves as

$$g(r, L) \asymp \begin{cases} r^{-2}, & r \leq \mathcal{O}(L/(\ln L)^{\hat{p}}) \\ L^{-2}(\ln L)^{\hat{p}}, & r \geq \mathcal{O}(L/(\ln L)^{\hat{p}}), \end{cases} \quad (12)$$

with $\hat{p} = 2\hat{y}_h = 1/2$. By (12), we explicitly point out that *no* multiplicative logarithmic correction appears in the r -dependence of $g(r, L) \asymp r^{-2}$, which is still Gaussian-like. By contrast, the plateau for $r \geq \xi_1 \sim L/(\ln L)^{\hat{p}}$ is modified as $L^{-2}(\ln L)^{\hat{p}}$. In other words, along any direction of the periodic hypercube, we have $g(r, L) \asymp r^{-2} + vL^{-2}(\ln L)^{\hat{p}}$, with v a non-universal constant. The decaying with r^{-2} at shorter distance in (12) is consistent with analytical calculations for the 4d weakly self-avoiding random walk and $O(n)$ ϕ^4 model directly in the thermodynamic limit ($L \rightarrow \infty$) [34], which predict $g(r) \asymp r^{-2}(1 + \mathcal{O}(1/\ln r))$.

The roles of terms with \tilde{f}_0 and \tilde{f}_1 in (11) are analogous to those in (9). The former arises from the Gaussian fixed point, and the latter describes the “background” contributions

($\mathbf{k} = 0$) for the FSS of macroscopic quantities. However, it is exact that the term with \tilde{f}_1 can no longer be regarded as an exact counterpart of the FSS of complete graph, due to the existence of multiplicative logarithmic corrections. By contrast, exact complete-graph mechanism applies to the \tilde{f}_1 term in (9), where logarithmic correction is absent and \tilde{f}_1 corresponds to the free energy of standard complete-graph model. According to (11), the FSS of various macroscopic quantities at $d = d_c$ can be obtained as

- the magnetization density $m \equiv L^{-d} \langle |\vec{\mathcal{M}}| \rangle \asymp L^{-1} (\ln L)^{\hat{y}_h} [1 + \mathcal{O}((\ln L)^{-\hat{y}_h})]$.
- the magnetic susceptibility $\chi_0 \asymp L^2 (\ln L)^{2\hat{y}_h} [1 + \mathcal{O}((\ln L)^{-2\hat{y}_h})]$.
- the magnetic fluctuations at $\mathbf{k} \neq 0$ Fourier modes $\chi_{\mathbf{k}} \asymp L^2$.
- the Binder cumulant Q may not take the exact complete-graph value, due to the multiplicative logarithmic correction. Some evidence was observed in a recent study by one of us (Y.D.) and his coworkers for the self-avoiding random walk ($n = 0$) on 4d periodic hypercubes, in which the maximum system size is up to $L = 700$.

The FSS of energy density, its higher-order fluctuations and the ℓ -moment Fourier modes at $\mathbf{k} \neq 0$ can be obtained.

In quantities like m and χ_0 , the FSS from the Gaussian fixed point effectively plays a role as finite-size corrections. Nevertheless, it is mentioned that in the analysis of numerical data, it is important to include such scaling terms.

We remark that the FSS formulae (11) and (12) for $d = d_c$ are less generic than (8) and (9) for $d > d_c$. For the $O(n)$ models, a multiplicative logarithmic correction is absent in the Gaussian r -dependence of $g(r, L)$ in (12). Albeit the two length scales is possibly a generic feature for models with logarithmic finite-size corrections at upper critical dimensionality, multiplicative logarithmic corrections to the r -dependence of $g(r, L)$ require case-by-case analyses. Formula (11) can be modified in some of these models, which include the percolation and spin-glass models in six dimensions.

We proceed to verify (11) and (12) using extensive Monte Carlo (MC) simulations of the $O(n)$ vector model. Before giving technical details, we present in Fig. 1 complementary evidence for (11) and (12) in the example of critical 4d XY model. Figure 1(a) shows the extensive data of $g(r, L)$ for $16 \leq L \leq 80$, of which the largest system contains about 4×10^7 lattice sites. To demonstrate the multiplicative logarithmic correction in the large-distance plateau indicated by (12), we plot $g(L/2, L)L^2$ versus $\ln L$ in the log-log scale in Fig. 1(b). The excellent agreement of the MC data with formula $v_1 (\ln L)^{1/2} + v_2$ provides a first-piece evidence for the presence of the logarithmic correction with exponent $\hat{p} = 1/2$. The second-piece evidence comes from Fig. 1(c), suggesting that the $\chi_0 L^{-2}$ data can be well described by formula $q_1 (\ln L)^{1/2} + q_2$. Finally, Fig. 1(d) plots the $\mathbf{k} \neq 0$ magnetic fluctuations χ_1 and χ_2 with $\mathbf{k}_1 = (2\pi/L, 0, 0, 0)$ and $\mathbf{k}_2 = (2\pi/L, 2\pi/L, 0, 0)$ respectively, which suppress the

L -dependent plateau and show the r -dependent behavior of $g(r, L)$. Indeed, the $\chi_1 L^{-2}$ and $\chi_2 L^{-2}$ data converge rapidly to constants as L increases.

III. NUMERICAL RESULTS AND FINITE-SIZE SCALING ANALYSES

Using a cluster MC algorithm [35], we simulate Hamiltonian (1) on 4d hypercubic lattices up to $L_{\max} = 96$ (Ising, XY) and 56 (Heisenberg), and measure a variety of macroscopic quantities including the magnetization density m , the susceptibility χ_0 , the magnetic fluctuations χ_1 and χ_2 , and the Binder cumulant Q . Moreover, we compute the two-point correlation function $g(r, L)$ for the XY model up to $L_{\max} = 90$ by means of a state-of-the-art worm MC algorithm [36].

A. Estimates of critical temperatures

In order to locate the critical temperatures T_c , we perform least-squares fits for the finite-size MC data of the Binder cumulant to

$$Q(L, T) = Q_c + a t L^{y_t} (\ln L)^{\hat{y}_t} + b (\ln L)^{-\hat{p}} + c \frac{\ln(\ln L)}{\ln L}, \quad (13)$$

where t is explicitly defined as $T_c - T$, Q_c is a universal ratio, and a, b, c are non-universal parameters. In addition to the leading additive logarithmic correction, we include $c \frac{\ln(\ln L)}{\ln L}$ proposed by [30] as a high-order correction, ensuring the stability of fits. In all fits, we justify the confidence by a standard manner: the fits with Chi squared χ^2 per degree of freedom (DF) is $\mathcal{O}(1)$ and remains stable as the cut-off size L_{\min} increases. The latter is for a caution against possible high-order corrections not included. The details of the fits are presented in the Supplemental Material (SM).

By analyzing the finite-size correction $Q(L, T_c) - Q_c$, we find that the leading correction is nearly proportional to $(\ln L)^{-1/2}$, consistent with the prediction of (11) and (12). We let Q_c be free in the fits and have $Q_c = 0.45(1)$, close to the complete-graph result $Q_c = 0.456\,947$. Besides, we perform simulations for the XY and Heisenberg models on the complete graph and obtain as $Q_c \approx 0.635$ and 0.728 , respectively, also close to the fitting results of the 4d Q data. We obtain $T_c(\text{XY}) = 3.314\,437(6)$, and Fig. 2(a) illustrates the location of T_c by Q .

We further examine the estimate of T_c by the FSS of other quantities such as the magnetization density m . For the XY model, Fig. 2(b) gives a log-log plot of the mL data versus $\ln L$ for $T = T_c$, as well as for $T_{\text{low}} = 3.314\,40$ and $T_{\text{above}} = 3.314\,50$. The significant bending-up and -down feature clearly suggests that $T_{\text{low}} < T_c$ and $T_{\text{above}} > T_c$, providing confidence for the finally quoted error margin of T_c .

The final estimates of T_c are summarized in Table I. For $n = 1$, we have $T_c = 6.680\,300(10)$, which is consonant with and improves over $T_c = 6.680\,263(23)$ [37] and marginally agrees with $T_c = 6.679\,63(36)$ [38] and $6.680\,339(14)$ [13]. For $n = 2$, our determination $T_c = 3.314\,437(6)$ significantly

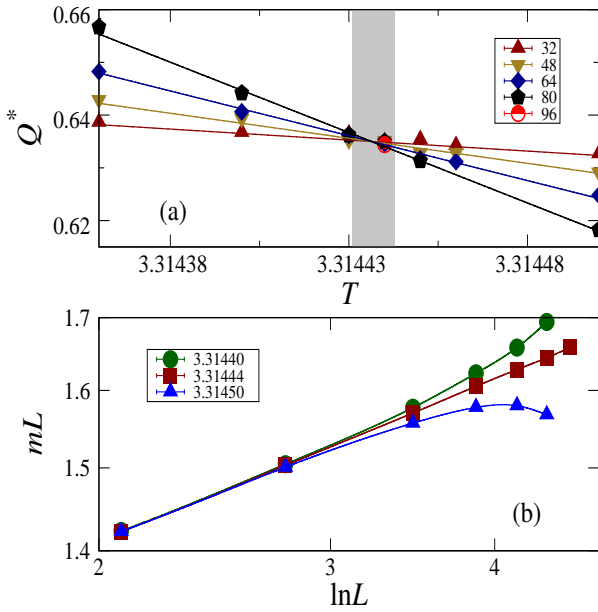


Figure 2. Locating T_c for the 4d XY model. (a) The Binder cumulant Q with finite-size corrections being subtracted, namely $Q^*(L, T) = Q(L, T) - b(\ln L)^{-\frac{1}{2}}$, with $b \approx 0.1069$ according to a preferred least-squares fit. The shadow marks T_c and its error margin. (b) The magnetization density m rescaled by L^{-1} versus $\ln L$ around $T_c = 3.31444$ in a log-log scale.

Table I. Estimates of T_c for the 4d $O(n)$ vector models.

Model	T_c	Ref.
	6.679 63(36)	[38]
Ising ($n = 1$)	6.680 339(14)	[13]
	6.680 263(23)	[37]
	6.680 300(10)	this work
XY ($n = 2$)	3.31, 3.314	[39–41]
	3.314 437(6)	this work
Heisenberg ($n = 3$)	2.192(1)	[42]
	2.198 79(2)	this work

improves over $T_c = 3.31$ [39, 40] and 3.314 [41]. For $n = 3$, our result $T_c = 2.19879(2)$ rules out $T_c = 2.192(1)$ from a high-temperature expansion [42].

B. Finite-size scaling of the two-point correlation

We then fit the critical two-point correlation $g(L/2, L)$ to

$$g(L/2, L) = v_1 L^{-2} (\ln L)^{\hat{p}} + v_2 L^{-2}, \quad (14)$$

where the first term comes from the large-distance plateau and the second one is from the r -dependent behavior of $g(r, L)$. With $\hat{p} = 1/2$ being fixed, the estimate of leading scaling term $L^{-1.98(4)}$ agrees well with the exact L^{-2} . With the exponent -2 in L^{-2} being fixed, the result $\hat{p} = 0.5(1)$ is also well consistent with the prediction $\hat{p} = 1/2$. These results are elaborated in the SM.

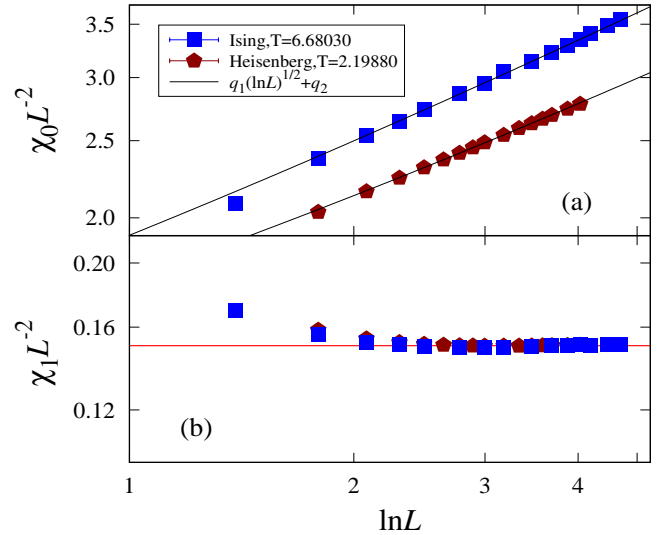


Figure 3. The magnetic fluctuations χ_0 (a) and χ_1 (b) rescaled by L^2 versus $\ln L$ in a log-log scale for the critical Ising and Heisenberg models. The black lines in (a) represent the least-squares fits, and the red one in (b) denotes a constant.

We remark that FSS analyses for $g(L/2, L)$ have already been performed in [16] with the formula $g(L/2, L) = AL^{-2}[\ln(L/2 + B)]^{1/2}$ (A and B are constants) and in [13] with a similar formula. These FSS in literature correspond to the first scaling term in Eq. (14). Hence, formula (14) serves as a forward step for complete FSS by involving the scaling term $v_2 L^{-2}$, which arises from the Gaussian fixed point.

C. Finite-size scaling of the magnetic susceptibility

According to (11) and (12), we fit the critical susceptibility χ_0 to

$$\chi_0 = q_1 L^2 (\ln L)^{\hat{p}} + q_2 L^2, \quad (15)$$

with q_1 and q_2 non-universal constants. For $\hat{p} = 1/2$ being fixed, we obtain fitting results with $\chi^2/\text{DF} \lesssim 1$ for each of $n = 1, 2, 3$, and correctly produce the leading scaling form L^2 . The scaled susceptibility $\chi_0 L^{-2}$ versus $\ln L$ are demonstrated by Figs. 1(c) (XY) and 3(a) (Ising and Heisenberg).

We note that previous studies based on a FSS without high-order corrections produced estimates of $\hat{y}_h (= \hat{p}/2)$, considered to be consistent with $\hat{y}_h = 1/4$ [38, 43–45]. The maximum lattice size therein was $L_{\max} = 24$, four times smaller than $L_{\max} = 96$ of the present study. In particular, it was reported [43] that $2\hat{y}_h = 0.45(8)$ and $4\hat{y}_h = 0.80(25)$. Nevertheless, we find that the fit $\chi_0 = q_1 L^2 (\ln L)^{2\hat{y}_h}$ by dropping the correction term $q_2 L^2$ would yield $\hat{y}_h = 0.21(1)$ (Ising), $0.20(1)$ (XY), and $0.19(1)$ (Heisenberg), which are smaller than and inconsistent with the predicted value $\hat{y}_h = 1/4$. This suggests the significance of $q_2 L^2$ in the susceptibility χ_0 , which arises from the r -dependence of $g(r, L)$.

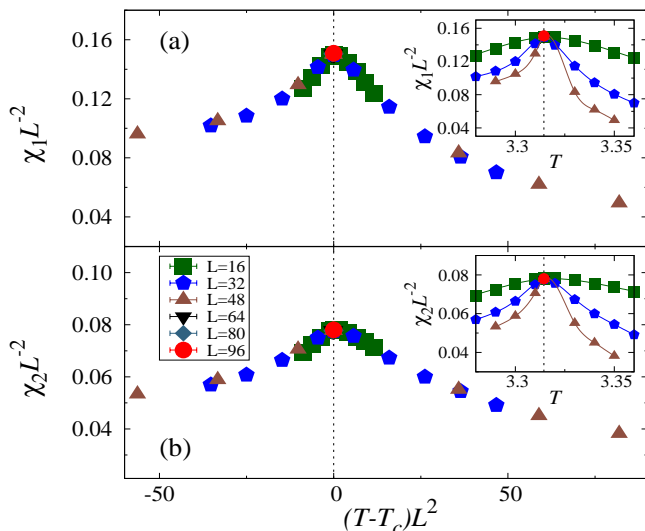


Figure 4. Data collapses for the magnetic fluctuations χ_1 (a) and χ_2 (b) rescaled by L^{2y_h-d} and L^{y_t} ($y_h = 3$, $y_t = 2$, $d = 4$) for the 4d XY model. The insets show the scaled fluctuations versus T , and the dashed lines denote T_c .

D. Finite-size scaling of the magnetic fluctuations at non-zero Fourier modes

We consider the magnetic fluctuations χ_1 with $|\mathbf{k}_1| = 2\pi/L$ and χ_2 with $|\mathbf{k}_2| = 2\sqrt{2}\pi/L$. We have compared the FSS of χ_0 , χ_1 and χ_2 in Figs. 1(c) and (d) for the critical 4d XY model. As L increases, $\chi_1 L^{-2}$ and $\chi_2 L^{-2}$ converge rapidly, suggesting the absence of multiplicative logarithmic correction. This is in sharp contrast to the behavior of $\chi_0 L^{-2}$, which diverges logarithmically. For the Ising and Heisenberg models, the FSS of the fluctuations at non-zero modes is also free of multiplicative logarithmic correction (Fig. 3(b)).

Surprisingly, it is found that the scaled fluctuations $\chi_1 L^{-2} \approx 0.15$ are equal within error bars for the Ising, XY, and Heisenberg models.

Further, we show in Fig. 4 χ_1 and χ_2 versus T for the 4d XY model. It is observed that the magnetic fluctuations at non-zero Fourier modes reach maximum at T_c and that the $\chi_1 L^{-2}$ ($\chi_2 L^{-2}$) data for different L s collapse well not only at T_c but also for a wide range of $(T - T_c)L^{y_t}$ with $y_t = 2$.

IV. DISCUSSIONS

We propose formulae (11) and (12) for the FSS of the $O(n)$ universality class at the upper critical dimensionality, which are tested against extensive MC simulations with $n = 1, 2, 3$. From the FSS of the magnetic fluctuations at zero and non-zero Fourier modes, the two-point correlation function, and the Binder cumulant, we obtain complementary and solid evidence supporting (11) and (12). As byproducts, the critical temperatures for $n = 1, 2, 3$ are all located up to an unprecedented precision.

An immediate application of (12) is to the massive amplitude excitation mode (often called the Anderson-Higgs boson) due to the spontaneous breaking of the continuous $O(n)$ symmetry [46], which is at the frontier of condensed matter research. At the pressure-induced quantum critical point (QCP) in the dimerized quantum antiferromagnet TiCuCl_3 , the 3D $O(3)$ amplitude mode was probed by neutron spectroscopy and a rather narrow peak width of about 15% of the excitation energy was revealed, giving no evidence for the logarithmic reduction of the width-mass ratio [3]. This was later confirmed by quantum MC study of a 3D model Hamiltonian of $O(3)$ symmetry [5, 6]. Indeed, (12) provides an explanation why the logarithmic-correction reduction in the Higgs resonance was not observed at 3D QCP. In numerical studies of the Higgs excitation mode at 3D QCP, the correlation function $g(\tau \equiv |\tau_1 - \tau_2|)$ is measured along the imaginary-time axis β , and numerical analytical continuation is used to deal with the $g(\tau)$ data. In practice, simulations are carried out at very low temperature $\beta \rightarrow \infty$, and it is expected that $g(\tau) \asymp \tau^{-2}$ for a significantly wide range of τ . Furthermore, it is the τ -dependent behavior of $g(\tau)$, instead of the L -dependence, that plays a decisive role in numerical analytical continuation.

In the thermodynamic limit, the two-point correlation function decays as $g(r) \sim r^{-2}\tilde{g}(r/\xi)$, where the scaling function $\tilde{g}(r/\xi)$ quickly drops to zero as $r/\xi \gg 1$. It can be seen that no multiplicative logarithmic correction exists in the algebraic decaying behavior. On the other hand, as the criticality is approached ($t \rightarrow 0$), the correlation length diverges as $\xi(t) \sim t^{-1/2}|\ln t|^{\hat{\nu}}$, and $\hat{\nu} = \frac{n+2}{2(n+8)} > 0$ implies that ξ diverges faster than $t^{-1/2}$ [30, 33]. Since the susceptibility can be calculated by summing up the correlation as $\chi_0 \sim \int_0^\xi g(r)r^{d-1}dr \sim \xi^2$, one has $\chi_0(t) \sim t^{-1}|\ln t|^{\hat{\gamma}}$ with $\hat{\gamma} = 2\hat{\nu}$. The thermodynamic scaling of $\chi_0(t)$ can also be obtained from the FSS formula (10) or (11), which gives $\chi_0(t, L) \sim L^{2y_h-4}(\ln L)^{2\hat{y}_h}\tilde{\chi}_0(tL^{y_t}(\ln L)^{\hat{y}_t})$. By fixing $tL^{y_t}(\ln L)^{\hat{y}_t}$ at some constant, one obtains the relation $L \sim t^{-1/y_t}|\ln t|^{-\hat{y}_t/y_t}$. Substituting it into the FSS of $\chi_0(t, L)$ yields $\chi_0(t) \sim t^\gamma|\ln t|^{\hat{\gamma}}$ with $\gamma = (2y_h - 4)/y_t$ and $\hat{\gamma} = -\gamma\hat{y}_t + 2\hat{y}_h$. With $(y_t, y_h, \hat{y}_t, \hat{y}_h) = (2, 3, \frac{4-n}{2n+16}, \frac{1}{4})$, one has $\gamma = 1$ and $\hat{\gamma} = \frac{n+2}{n+8}$. The thermodynamic scaling with logarithmic corrections has been demonstrated in Ref. [4] in terms of the magnetization m of an $O(3)$ Hamiltonian.

For the critical Ising model in five dimensions, an unwrapped distance r_u was introduced to account for the winding numbers across a finite torus [18]. The unwrapped correlation was shown to behave as $g(r_u) \sim r_u^{2-d}\tilde{g}(r_u/\xi_u)$, where the unwrapped correlation length diverges as $\xi_u \sim L^{d/4}$. This differs from typical correlation functions that are cut off by the linear system size $\sim L$. We expect that at $d_c = 4$, the unwrapped correlation length diverges as $\xi_u \sim L(\ln L)^{\hat{y}_h}$, which gives the critical susceptibility as $\chi_0(L) \sim L^2(\ln L)^{2\hat{y}_h}$.

Besides, formula (12) is useful for predicting various critical behaviors. As an instance, it was observed that an impurity immersed in a 2D $O(2)$ quantum critical environment can evolve into a quasiparticle of fractionalized charge, as the impurity-environment interaction is tuned to a boundary crit-

ical point [47–49]. Formula (12) precludes the emergence of such a quantum-fluctuation-induced quasiparticle at 3D O(2) QCP.

We mention an open question about the specific heat of the 4d Ising model. FSS formula (10) predicts that the critical specific heat diverges as $C \asymp (\ln L)^{1/3}$. By contrast, a MC study demonstrated that the critical specific heat is bounded [37]. The complete scaling form (11) is potentially useful for reconciling the inconsistency.

Finally, it would be possible to extend the present scheme to other systems of critical phenomena, as the existence of upper critical dimensionality is a common feature therein. These systems include the percolation and spin-glass models at their upper critical dimensionality $d_c = 6$. We leave this for a future study.

V. METHOD

Throughout the paper, the raw data for any temperature T and linear size L are obtained by means of MC simulations, for which the Wolff cluster algorithm [35] and the Prokof’ev-Svistunov worm algorithm [36] are employed complementarily. Both algorithms are state-of-the-art tools in their own territories.

The O(n) vector model (1) in its original spin representation is efficiently sampled by the Wolff cluster algorithm, which is the single-cluster version of the widely utilized non-local cluster algorithms. The present study uses the standard procedure of the algorithm, as in the original paper [35] where the algorithm was invented. In some situations, we also use the conventional Metropolis algorithm [50] for benchmarks. The

macroscopic physical quantities of interest have been introduced in aforementioned sections for the spin representation.

The two-point correlation function for the XY model ($n = 2$) is sampled by means of the Prokof’ev-Svistunov worm algorithm, which was invented for a variety of classical statistical models [36]. By means of a high-temperature expansion, we perform an exact transformation for the original XY spin model to a graphic model in directed-flow representation. We then introduce two defects for enlarging the state space of directed flows. The Markov chain process of evolution is built upon biased random walks of defects, which satisfy the detailed balance condition. It is defined that the evolution hits the original directed-flow state space when the two defects meet at a site. The details for the exact transformation and a step-by-step procedure for the algorithm have been presented in a recent reference [51].

ACKNOWLEDGMENTS

Acknowledgements. YD is indebted to valuable discussions with Timothy Garoni, Jens Grimm and Zongzheng Zhou. This work has been supported by the National Natural Science Foundation of China under Grants No. 11774002, No. 11625522, and No. 11975024, the National Key R&D Program of China under Grants No. 2016YFA0301604 and No. 2018YFA0306501, and the Department of Education in Anhui Province.

VI. CONFLICT OF INTEREST STATEMENT

None declared.

-
- [1] R. Fernández, J. Fröhlich, and A. D. Sokal, *Random walks, critical phenomena, and triviality in quantum field theory* (Springer, Berlin, 2013).
- [2] B. V. Svistunov, E. S. Babaev, and N. V. Prokof’ev, *Superfluid states of matter* (CRC Press, London, 2015).
- [3] P. Merchant, B. Normand, K. W. Krämer, M. Boehm, D. F. McMorrow, and Ch. Rüegg, “Quantum and classical criticality in a dimerized quantum antiferromagnet,” *Nat. Phys.* **10**, 373–379 (2014).
- [4] Y. Q. Qin, B. Normand, A. W. Sandvik, and Z. Y. Meng, “Multiplicative logarithmic corrections to quantum criticality in three-dimensional dimerized antiferromagnets,” *Phys. Rev. B* **92**, 214401 (2015).
- [5] M. Lohöfer and S. Wessel, “Excitation-gap scaling near quantum critical three-dimensional antiferromagnets,” *Phys. Rev. Lett.* **118**, 147206 (2017).
- [6] Y. Q. Qin, B. Normand, A. W. Sandvik, and Z. Y. Meng, “Amplitude mode in three-dimensional dimerized antiferromagnets,” *Phys. Rev. Lett.* **118**, 147207 (2017).
- [7] Y. Cui, H. Zou, N. Xi, Z. He, Y. X. Yang, L. Shu, G. H. Zhang, Z. Hu, T. Chen, R. Yu, J. Wu, and W. Yu, “Quantum criticality of the ising-like screw chain antiferromagnet $\text{SrCo}_2\text{V}_2\text{O}_8$ in a transverse magnetic field,” *Phys. Rev. Lett.* **123**, 067203 (2019).
- [8] D. J. Resnick, J. C. Garland, J. T. Boyd, S. Shoemaker, and R. S. Newrock, “Kosterlitz-thouless transition in proximity-coupled superconducting arrays,” *Phys. Rev. Lett.* **47**, 1542–1545 (1981).
- [9] A. Goldman, *Percolation, localization, and superconductivity*, Vol. 109 (Springer, Boston, 2013).
- [10] M. Greiner, O. Mandel, T. Esslinger, T. W. Hänsch, and I. Bloch, “Quantum phase transition from a superfluid to a mott insulator in a gas of ultracold atoms,” *Nature* **415**, 39–44 (2002).
- [11] B. Capogrosso-Sansone, N. V. Prokof’ev, and B. V. Svistunov, “Phase diagram and thermodynamics of the three-dimensional bose-hubbard model,” *Phys. Rev. B* **75**, 134302 (2007).
- [12] J. Cardy, *Finite-size scaling*, Vol. 2 (Elsevier, Amsterdam, 2012).
- [13] E. Luijten, *Interaction range, universality and the upper critical dimension* (Delft University Press, Delft, 1997).
- [14] E. Luijten, K. Binder, and H. W. J. Blöte, “Finite-size scaling above the upper critical dimension revisited: the case of the five-dimensional ising model,” *Euro. Phys. J. B* **9**, 289–297 (1999).

- [15] M. Wittmann and A. P. Young, “Finite-size scaling above the upper critical dimension,” *Phys. Rev. E* **90**, 062137 (2014).
- [16] R. Kenna and B. Berche, “Fisher’s scaling relation above the upper critical dimension,” *EPL (Europhysics Letters)* **105**, 26005 (2014).
- [17] E. Flores-Sola, B. Berche, R. Kenna, and M. Weigel, “Role of fourier modes in finite-size scaling above the upper critical dimension,” *Phys. Rev. Lett.* **116**, 115701 (2016).
- [18] J. Grimm, E. M. Elçi, Z. Zhou, T. M. Garoni, and Y. Deng, “Geometric explanation of anomalous finite-size scaling in high dimensions,” *Phys. Rev. Lett.* **118**, 115701 (2017).
- [19] V. Papanthakos, *Finite-size effects in high-dimensional statistical mechanical systems: The Ising model with periodic boundary conditions* (Ph.D. thesis, Princeton University, Princeton, New Jersey, 2006).
- [20] Z. Zhou, J. Grimm, S. Fang, Y. Deng, and T. M. Garoni, “Random-length random walks and finite-size scaling in high dimensions,” *Phys. Rev. Lett.* **121**, 185701 (2018).
- [21] S. Fang, J. Grimm, Z. Zhou, and Y. Deng, “Anomalous finite-size scaling in the fortuin-kasteleyn clusters of the five-dimensional ising model with periodic boundary conditions,” [arXiv:1909.04328](https://arxiv.org/abs/1909.04328) (2019).
- [22] M. E. Fisher, *Critical Phenomena, Proceedings of the 51st Enrico Fermi Summer School, Varenna, Italy, edited by M. S. Green* (Academic, New York, 1971).
- [23] K. Binder, M. Nauenberg, V. Privman, and A. P. Young, “Finite-size tests of hyperscaling,” *Phys. Rev. B* **31**, 1498 (1985).
- [24] B. Berche, R. Kenna, and J.-C. Walter, “Hyperscaling above the upper critical dimension,” *Nucl. Phys. B* **865**, 115–132 (2012).
- [25] R. Kenna and B. Berche, “A new critical exponent kappa and its logarithmic counterpart kappa-hat,” *Cond. Matt. Phys.* **16**, 23601 (2013).
- [26] M. Aizenman, “Geometric analysis of φ^4 fields and ising models. parts i and ii,” *Commun. Math. Phys.* **86**, 1–48 (1982).
- [27] M. Aizenman, *Rigorous studies of critical behavior II, Statistical Physics and Dynamical Systems: Rigorous Results, edited by J. Fritz, A. Jaffe, D. Szasz*. (Birkhauser, Boston, 1985).
- [28] M. Aizenman, “Rigorous studies of critical behavior,” *Physica A* **140**, 225–231 (1986).
- [29] W. Huang, P. Hou, J. Wang, R. M. Ziff, and Y. Deng, “Critical percolation clusters in seven dimensions and on a complete graph,” *Phys. Rev. E* **97**, 022107 (2018).
- [30] R. Kenna, “Finite size scaling for $o(n)$ ϕ^4 -theory at the upper critical dimension,” *Nucl. Phys. B* **691**, 292–304 (2004).
- [31] N. Aktekin, “The finite-size scaling functions of the four-dimensional ising model,” *J. Stat. Phys.* **104**, 1397–1406 (2001).
- [32] F. J. Wegner and E. K. Riedel, “Logarithmic corrections to the molecular-field behavior of critical and tricritical systems,” *Phys. Rev. B* **7**, 248 (1973).
- [33] R. Kenna, *Universal scaling relations for logarithmic-correction exponents, Order, Disorder and Criticality, Advanced Problems of Phase Transition Theory, edited by Y. Holovatch* (World Scientific, New York, 2012).
- [34] G. Slade and A. Tomberg, “Critical correlation functions for the 4-dimensional weakly self-avoiding walk and n-component ϕ^4 model,” *Commun. Math. Phys.* **342**, 675–737 (2016).
- [35] U. Wolff, “Collective monte carlo updating for spin systems,” *Phys. Rev. Lett.* **62**, 361 (1989).
- [36] N. V. Prokof’ev and B. V. Svistunov, “Worm algorithms for classical statistical models,” *Phys. Rev. Lett.* **87**, 160601 (2001).
- [37] P. H. Lundow and K. Markström, “Critical behavior of the ising model on the four-dimensional cubic lattice,” *Phys. Rev. E* **80**, 031104 (2009).
- [38] R. Kenna and C. B. Lang, “Finite size scaling and the zeroes of the partition function in the ϕ_4^4 model,” *Phys. Lett. B* **264**, 396–400 (1991).
- [39] L. M. Jensen, B. J. Kim, and P. Minnhagen, “Critical dynamics of the four-dimensional xy model,” *Physica B* **284**, 455–456 (2000).
- [40] L. M. Jensen, B. J. Kim, and P. Minnhagen, “Dynamic critical exponent of two-, three-, and four-dimensional xy models with relaxational and resistively shunted junction dynamics,” *Phys. Rev. B* **61**, 15412 (2000).
- [41] Y. Nonomura and Y. Tomita, “Critical nonequilibrium relaxation in the swendsen-wang algorithm in the berezinsky-kosterlitz-thouless and weak first-order phase transitions,” *Phys. Rev. E* **92**, 062121 (2015).
- [42] S. McKenzie, C. Domb, and D. L. Hunter, “The high-temperature susceptibility of the classical heisenberg model in four dimensions,” *J Phys A: Math. Gen.* **15**, 3909–3914 (1982).
- [43] P.-Y. Lai and K. K. Mon, “Finite-size scaling of the ising model in four dimensions,” *Phys. Rev. B* **41**, 9257 (1990).
- [44] R. Kenna and C. B. Lang, “Renormalization group analysis of finite-size scaling in the ϕ_4^4 model,” *Nucl. Phys. B* **393**, 461–479 (1993).
- [45] R. Kenna and C. B. Lang, “Scaling and density of lee-yang zeros in the four-dimensional ising model,” *Phys. Rev. E* **49**, 5012 (1994).
- [46] D. Pekker and C. M. Varma, “Amplitude/higgs modes in condensed matter physics,” *Annu. Rev. Condens. Matter Phys.* **6**, 269–297 (2015).
- [47] Y. Huang, K. Chen, Y. Deng, and B. Svistunov, “Trapping centers at the superfluid–mott-insulator criticality: Transition between charge-quantized states,” *Phys. Rev. B* **94**, 220502 (2016).
- [48] S. Whitsitt and S. Sachdev, “Critical behavior of an impurity at the boson superfluid–mott-insulator transition,” *Phys. Rev. A* **96**, 053620 (2017).
- [49] K. Chen, Y. Huang, Y. Deng, and B. Svistunov, “Halon: A quasiparticle featuring critical charge fractionalization,” *Phys. Rev. B* **98**, 214516 (2018).
- [50] N. Metropolis, A. W. Rosenbluth, M. N. Rosenbluth, A. H. Teller, and E. Teller, “Equation of state calculations by fast computing machines,” *J. Chem. Phys.* **21**, 1087–1092 (1953).
- [51] W. Xu, Y. Sun, J.-P. Lv, and Y. Deng, “High-precision monte carlo study of several models in the three-dimensional $u(1)$ universality class,” *Phys. Rev. B* **100**, 064525 (2019).

Supplemental Material for “Finite-size Scaling of $O(n)$ Systems at the Upper Critical Dimensionality”

Jian-Ping Lv,^{1,*} Wanwan Xu,¹ Yanan Sun,¹ Kun Chen,^{2,†} and Youjin Deng^{3,4,‡}

¹*Department of Physics, Anhui Key Laboratory of Optoelectric Materials Science and Technology, Key Laboratory of Functional Molecular Solids, Ministry of Education, Anhui Normal University, Wuhu, Anhui 241000, China*

²*Department of Physics and Astronomy, Rutgers, The State University of New Jersey, Piscataway, New Jersey 08854-8019*

³*National Laboratory for Physical Sciences at Microscale and Department of Modern Physics, University of Science and Technology of China, Hefei, Anhui 230026, China*

⁴*Department of Physics and Electronic Information Engineering, Minjiang University, Fuzhou, Fujian 350108, China*

(Dated: September 23, 2020)

We elaborate the quantifications of the finite-size scaling (FSS) mentioned in the main text. Subsequently, we address the location of the critical temperatures T_c , the FSS of the susceptibility χ_0 , and the FSS of the two-point correlation $g(r, L)$ with $r = L/2$.

THE ESTIMATE OF T_c

For each of the four-dimensional Ising, XY, and Heisenberg models, the estimate of T_c is achieved by fitting the finite-size Monte Carlo data of the Binder cumulant Q to the scaling ansatz

$$Q(L, T) = Q_c + atL^{y_t}(\ln L)^{\hat{y}_t} + b(\ln L)^{-\hat{p}} + c \frac{\ln(\ln L)}{\ln L} \quad (1)$$

where $t \equiv T_c - T$, for $t \rightarrow 0$. Q_c is the critical dimensionless ratio and a, b, c are constants. In the fits, the mean-field thermal exponent is fixed as $y_t = 2$ for reducing uncertainty.

For the Ising model, as shown in Table I, we perform fits with \hat{y}_t being fixed to be $\hat{y}_t = \frac{4-n}{2n+16} = 1/6$ as predicated by renormalization-group calculations [1] or being free. After obtaining an estimate of T_c , we also perform fits right at T_c . Stable fits with $\chi^2/\text{DF} \approx 1$ are achieved for all of these scenarios. As we let Q_c free, it is found $Q_c = 0.45(1)$, which is close to $Q_c = 0.456947$ of the complete-graph model [2]. By these fits, we estimate $\hat{p} \approx 0.5$. The fits for Q of the XY and Heisenberg models are summarized in Tables II and III, where the estimates for Q_c are again close to the results $Q_c \approx 0.635$ and 0.728 by Monte Carlo simulations of XY and Heisenberg models on complete graph [3], respectively. Meanwhile, we note that the amplitude of correction $b \approx 0.1$ is sizeable for each of the four-dimensional models. Hence, the prediction of this study on the existence of the finite-size correction $b(\ln L)^{-\hat{p}}$ is further confirmed. This correction form is visualized by Fig. 1 for the Ising, XY, and Heisenberg models. The locating of T_c is shown in Fig. 2.

The final estimates of T_c are determined by comparing the fits, and are $T_c = 6.68030(1)$, $3.314437(6)$, and $2.19879(2)$, for the Ising, XY, and Heisenberg models, respectively. These estimates can be examined independently using the quantities other than Q , e.g., the magnetization density m . Figure 3 displays m rescaled by the mean-field factor L^{y_h-d} ($y_h = 3$,

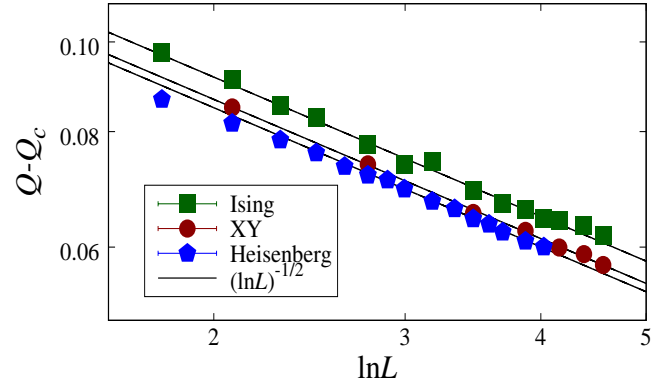


Figure 1. Finite-size corrections $Q(L, T_c) - Q_c$ of the Binder cumulant Q versus $\ln L$ in a log-log scale for the critical Ising, XY, and Heisenberg models. The solid lines are drawn according to preferred fits and stand for the $(\ln L)^{-\frac{1}{2}}$ decaying.

$d = 4$) versus $\ln L$ in a log-log scale around T_c for the Ising, XY, and Heisenberg models. The linearities at T_c in the plots confirm that the estimated T_c are reasonable for the present lattice size scale, while the bending-up or -down features with respect to the linearities suggest the deviations from T_c . For the Ising model, we confirm the linearity at $T_c = 6.68030$, and preclude the temperatures $T = 6.680263$ and 6.68060 as T_c . For the XY model, we confirm $T_c = 3.31444$, and preclude $T_c = 3.31440$ and 3.31450 . For the Heisenberg model, $T_c = 2.19880$ is confirmed and $T_c = 2.19867$ and 2.19887 are both precluded.

FSS OF THE SUSCEPTIBILITY χ_0

We fit the Monte Carlo data of the susceptibility χ_0 at T_c to the ansatz

$$\chi_0(L, T_c) = q_1 L^{2y_h-d} (\ln L)^{\hat{p}} + q_2 L^{2y_h-d}, \quad (2)$$

which is an inference drawn from the scaling formulae of free energy density and two-point correlation. The fits are summarized in Table IV for the critical Ising, XY, and Heisenberg models. For each of the models, we confirm that, if one in-

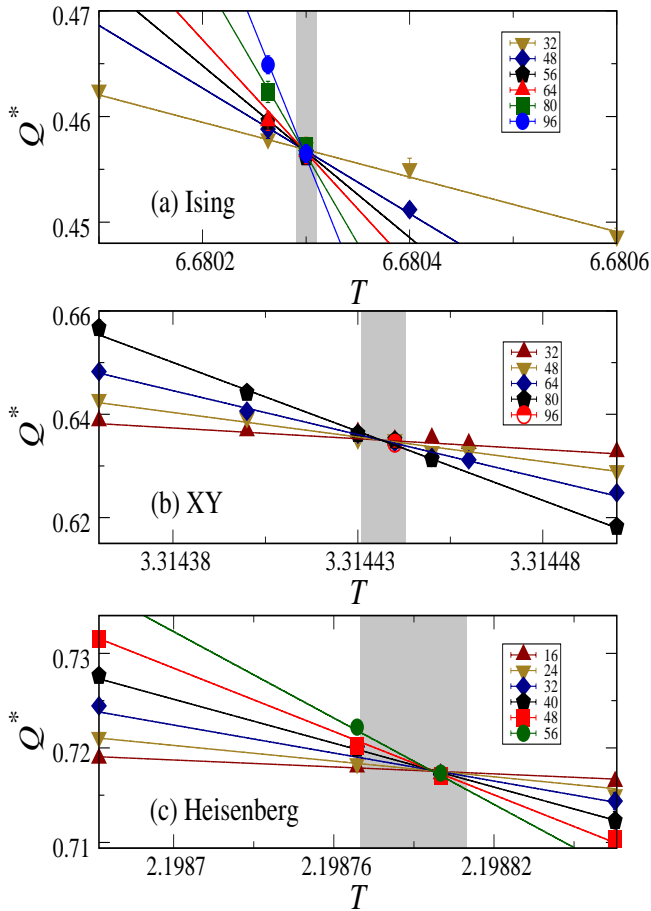


Figure 2. The Binder cumulant Q with finite-size corrections being subtracted, namely $Q^*(L, T) = Q(L, T) - b(\ln L)^{-\frac{1}{2}}$, with $b \approx 0.0991, 0.1069, \text{ and } 0.1160$ according to the preferred least-squares fits for the Ising (a), XY (b), and Heisenberg (c) models, respectively. The solid lines are drawn according to the fits, and the shadows mark T_c and their error margins. The plot for the XY case has appeared in the main text and we hereby include it for completeness.

cludes both q_1 and q_2 terms and let $\hat{p} = 1/2$ and $2y_h - d = 2$ fixed, stable fits with $\chi^2/\text{DF} \lesssim 1$ can be achieved. If the mean-field exponent $2y_h - d$ is free in the fits, we obtain $2y_h - d \approx 2.00$ for each model, in perfect agreement with the exact value 2 within error bars. For the Ising and XY models (for which we have Monte Carlo data with $L_{\max} = 96$), we achieve stable fits with \hat{p} being free, which yield $\hat{p} \approx 0.5$, consistent with the prediction $\hat{p} = 1/2$.

FSS OF THE TWO-POINT CORRELATION $g(L/2, L)$

We perform FSS for the large-distance plateau of two-point correlation $g(r, L)$, by fitting the finite-size $g(L/2, L)$ data to the ansatz

$$g(L/2, L) = v_1 L^{2y_h - 2d} (\ln L)^{\hat{p}} + v_2 L^{2y_h - 2d} \quad (3)$$

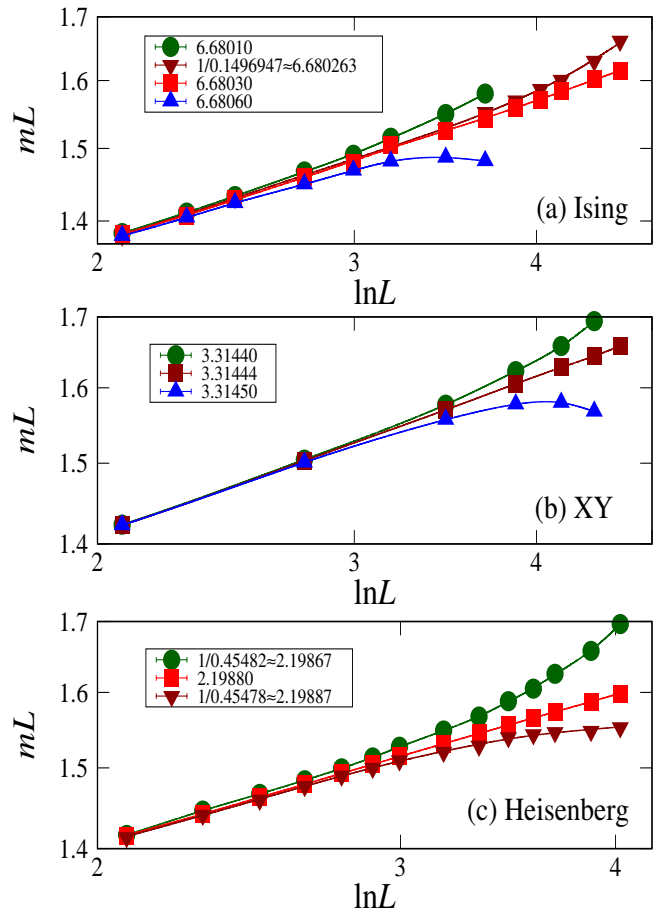


Figure 3. The magnetization density m rescaled by its mean-field factor $L^{y_h - d}$ ($y_h = 3, d = 4$) versus $\ln L$ around $T_c = 6.68030, 3.31444, \text{ and } 2.19880$ in a log-log scale, for the Ising (a), XY (b), and Heisenberg (c) models, respectively. For each of the models, linearity is observed at T_c , and the bending-up or -down feature with respect to the linearity indicates the deviation from criticality. The plot for the XY case has appeared in the main text and we hereby include it for completeness.

for the critical XY model. We perform fits under the situations that $2y_h - 2d = -2$ and $\hat{p} = 1/2$ are both fixed, and that only one of them is fixed. The fits are summarized by Table V, which demonstrates that the inclusion of both v_1 and v_2 terms correctly produces the mean-field exponent y_h . As an instance, one of the fits yields $2y_h - 2d = -1.99(1)$ with $L_{\min} = 24$ and $\chi^2/\text{DF} \approx 0.8$, which is in good agreement with the exact $2y_h - 2d = -2$. By comparing the fits with $\hat{p} = 1/2$ being fixed, we estimate $y_h = 3.01(2)$. As a further verification, once the mean-field exponent $2y_h - 2d = -2$ is fixed, the estimate $\hat{p} = 0.5(1)$ is again consistent with the prediction $\hat{p} = 1/2$.

* jplv2014@ahnu.edu.cn
† chenkun0228@gmail.com
‡ yjdeng@ustc.edu.cn

- [1] R. Kenna, “Universal scaling relations for logarithmic-correction exponents,” Chapter 1, Order, Disorder and Criticality, Advanced Problems of Phase Transition Theory, Vol. 3, Y. Holovatch ed (World Scientific, 2012).
- [2] E. Luijten, *Interaction range, universality and the upper critical dimension* (Delft University Press, 1997).
- [3] M.-H. Hu and J.-P. Lv, unpublished results (2019).

Table I. Fits of the finite-size Monte Carlo data of the Binder cumulant Q to (1) for the Ising ($n = 1$) model. The missing entries mean that the corresponding high-order corrections are not included or that the fits are performed right at $T_c = 6.680\ 30$.

L_{\min}	χ^2/DF	T_c	\hat{y}_t	\hat{p}	Q_c	a	b	c
8	61.6/45	6.680 310(6)	-0.3(2)	0.5(1)	0.44(2)	0.04(1)	0.13(1)	
32	9.0/16	6.680 307(9)	-0.5(5)	0.6(1)	0.456947	0.05(3)	0.12(1)	
32	10.7/17	6.680 302(6)	1/6	0.59(9)	0.456947	0.0205(8)	0.11(1)	
40	9.2/12	6.680 302(9)	1/6	0.6(2)	0.456947	0.020(1)	0.11(3)	
24	34.1/22	6.680 292(2)	1/6	0.5	0.456947	0.0207(8)	0.1004(3)	
32	11.6/18	6.680 297(3)	1/6	0.5	0.456947	0.0206(8)	0.0991(5)	
40	9.4/13	6.680 298(3)	1/6	0.5	0.456947	0.020(1)	0.0987(6)	
48	2.0/8	6.680 301(4)	1/6	0.5	0.456947	0.019(1)	0.098(1)	
56	1.7/5	6.680 302(5)	1/6	0.5	0.456947	0.019(2)	0.098(1)	
24	18.8/22	6.680 307(4)	1/6	0.5	0.456947	0.0203(8)	0.17(1)	-0.11(2)
32	10.7/17	6.680 301(5)	1/6	0.5	0.456947	0.0205(8)	0.13(3)	-0.05(5)
40	9.2/12	6.680 302(8)	1/6	0.5	0.456947	0.020(1)	0.13(7)	0.0(1)
12	14.8/8			0.5	0.441(2)		0.130(3)	
16	6.2/7			0.5	0.446(3)		0.119(5)	
20	2.8/6			0.5	0.451(4)		0.110(7)	
32	1.8/5			0.5	0.457(7)		0.10(1)	
40	1.2/4			0.5	0.460(8)		0.09(2)	
8	10.1/9			0.5	0.460(5)		0.137(2)	-0.06(2)
20	2.6/6			0.56(3)	0.456947		0.107(5)	
32	1.8/5			0.50(7)	0.456947		0.099(9)	
8	10.1/9			0.48(4)	0.456947		0.140(6)	-0.07(2)

Table II. Fits of the finite-size Monte Carlo data of the Binder cumulant Q to (1) for the XY ($n = 2$) model. The missing entries mean that the corresponding high-order corrections are not included or that the fits are performed right at $T_c = 3.314\ 44$.

L_{\min}	χ^2/DF	T_c	\hat{y}_t	\hat{p}	Q_c	a	b	c
8	29.9/35	3.314 440(3)	-0.2(3)	0.5(1)	0.62(3)	0.05(2)	0.13(2)	
8	30.6/36	3.314 440(3)	1/10	0.5(1)	0.62(3)	0.0360(8)	0.13(2)	
8	30.7/37	3.314 439(2)	1/10	0.5	0.63(1)	0.0360(8)	0.126(2)	
16	25.8/30	3.314 439(2)	1/10	0.5	0.62(1)	0.0360(8)	0.126(4)	
32	23.6/23	3.314 442(4)	1/10	0.5	0.62(1)	0.0360(8)	0.13(1)	
16	50.4/31	3.314 430(1)	1/10	0.5	0.635	0.0358(8)	0.1091(2)	
32	26.9/24	3.314 434(1)	1/10	0.5	0.635	0.0359(8)	0.1078(3)	
48	18.1/17	3.314 436(2)	1/10	0.5	0.635	0.0360(8)	0.1069(7)	
16	26.4/30	3.314 437(2)	1/10	0.5	0.635	0.0360(8)	0.131(4)	-0.035(7)
32	23.7/23	3.314 440(4)	1/10	0.5	0.635	0.0360(8)	0.15(3)	-0.07(4)
8	1.9/5			0.5	0.63(1)		0.123(2)	
16	1.9/4			0.5	0.63(1)		0.123(4)	
32	0.8/3			0.5	0.63(1)		0.11(1)	
8	1.9/4			0.5(2)	0.63(2)		0.12(2)	
32	0.8/3			0.53(5)	0.635		0.111(7)	
48	0.6/2			0.6(1)	0.635		0.12(2)	
8	1.8/4			0.59(9)	0.635		0.114(8)	0.01(3)
16	1.0/3			0.4(1)	0.635		0.15(4)	-0.07(9)

Table III. Fits of the finite-size Monte Carlo data of the Binder cumulant Q to (1) for the Heisenberg ($n = 3$) model. The missing entries mean that the corresponding high-order corrections are not included or that the fits are performed right at $T_c = 2.198\ 80$.

L_{\min}	χ^2/DF	T_c	\hat{y}_t	\hat{p}	Q_c	a	b	c
24	22.4/24	2.198 796(8)	1/22	0.59(7)	0.728	0.045(1)	0.108(9)	
12	41.0/44	2.198 791(3)	1/22	0.5	0.72(1)	0.045(1)	0.108(2)	
16	32.7/36	2.198 796(4)	1/22	0.5	0.72(1)	0.046(1)	0.114(5)	
20	25.4/28	2.198 799(6)	1/22	0.5	0.72(1)	0.046(1)	0.118(8)	
24	22.4/24	2.198 797(8)	1/22	0.5	0.72(1)	0.045(1)	0.11(1)	
20	31.2/29	2.198 785(2)	1/22	0.5	0.728	0.045(1)	0.0981(2)	
24	23.9/25	2.198 788(2)	1/22	0.5	0.728	0.045(1)	0.0976(3)	
32	20.9/17	2.198 789(3)	1/22	0.5	0.728	0.045(1)	0.0974(5)	
12	42.3/44	2.198 788(3)	1/22	0.5	0.728	0.045(1)	0.108(2)	-0.015(4)
16	33.5/36	2.198 793(4)	1/22	0.5	0.728	0.046(1)	0.116(5)	-0.028(9)
20	25.6/28	2.198 795(5)	1/22	0.5	0.728	0.046(1)	0.12(1)	-0.04(2)
24	22.6/24	2.198 795(7)	1/22	0.5	0.728	0.045(1)	0.12(2)	-0.03(3)
16	8.0/8			0.5	0.72(1)		0.120(3)	
20	2.6/6			0.5	0.71(1)		0.121(4)	
24	2.5/5			0.5	0.71(1)		0.122(6)	
32	0.9/3			0.5	0.71(1)		0.12(1)	
12	10.4/9			0.5	0.70(1)		0.111(4)	0.04(3)
16	6.8/7			0.5	0.70(1)		0.11(1)	0.06(5)
20	2.3/5			0.5	0.70(2)		0.11(2)	0.1(1)
24	2.3/4			0.5	0.70(4)		0.10(5)	0.1(2)

Table IV. Fits of the finite-size Monte Carlo data of the magnetic susceptibility χ_0 to (2) for the critical Ising ($n = 1$), XY ($n = 2$) and Heisenberg ($n = 3$) models.

n	L_{\min}	χ^2/DF	$2y_h - d$	\hat{p}	q_1	q_2
1	8	6.3/9	2	0.56(4)	1.2(1)	0.7(2)
	10	5.0/8	2	0.50(7)	1.4(3)	0.5(3)
	12	1.3/7	2	0.6(1)	1.0(3)	1.0(3)
	8	8.2/10	2	0.5	1.440(6)	0.46(1)
	10	5.0/9	2	0.5	1.448(8)	0.45(1)
	12	3.4/8	2	0.5	1.44(1)	0.46(2)
	16	2.7/7	2	0.5	1.45(1)	0.45(3)
	20	0.8/6	2	0.5	1.47(2)	0.40(4)
	8	6.2/9	2.006(5)	0.5	1.35(6)	0.56(7)
	10	5.0/8	2.001(7)	0.5	1.4(1)	0.5(1)
	12	1.3/7	2.01(1)	0.5	1.2(1)	0.7(2)
	16	1.1/6	2.02(1)	0.5	1.2(2)	0.8(3)
	20	0.6/5	2.01(2)	0.5	1.3(3)	0.6(4)
	2	8	0.6/4	2	0.45(4)	1.5(2)
16		0.2/3	2	0.4(1)	2(1)	0(1)
8		1.8/5	2	0.5	1.254(6)	0.49(1)
16		1.1/4	2	0.5	1.25(1)	0.50(2)
32		0.4/3	2	0.5	1.23(2)	0.54(5)
48		0.1/2	2	0.5	1.21(4)	0.58(9)
8		0.5/4	1.995(4)	0.5	1.32(6)	0.41(7)
16		0.2/3	1.99(1)	0.5	1.4(2)	0.3(2)
3	10	26.1/11	2	0.5	1.109(3)	0.565(5)
	12	13.4/10	2	0.5	1.100(4)	0.581(7)
	16	8.1/8	2	0.5	1.089(6)	0.60(1)
	20	4.0/6	2	0.5	1.075(9)	0.63(2)
	24	4.0/5	2	0.5	1.07(1)	0.63(3)
	28	0.5/4	2	0.5	1.05(2)	0.68(4)
	32	0.4/3	2	0.5	1.06(3)	0.66(5)
	16	3.3/7	1.98(1)	0.5	1.4(1)	0.2(2)
	20	2.9/5	1.98(2)	0.5	1.3(2)	0.3(3)

Table V. Fits of the finite-size Monte Carlo data of the two-point correlation $g(L/2, L)$ to (3) for the critical XY model.

L_{\min}	χ^2/DF	$2y_h - 2d$	\hat{p}	v_1	v_2
24	4.0/5	-2	0.5	0.607(3)	0.339(6)
32	2.2/4	-2	0.5	0.613(6)	0.33(1)
40	1.5/3	-2	0.5	0.61(1)	0.34(2)
24	3.3/4	-1.99(1)	0.5	0.54(8)	0.42(9)
32	1.3/3	-2.02(2)	0.5	0.8(2)	0.1(3)
40	1.3/2	-2.02(4)	0.5	0.8(4)	0.1(6)
16	28.5/5	-2	0.52(5)	0.55(8)	0.41(9)
24	4.8/4	-2	0.5(1)	0.7(3)	0.2(3)